

1994 NASA/ASEE SUMMER FACULTY FELLOWSHIP PROGRAM

117 759

JOHN F. KENNEDY SPACE CENTER  
UNIVERSITY OF CENTRAL FLORIDA

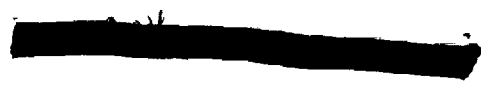
58.47

33968

p- 29

LIGHTNING STUDIES USING LDAR AND  
COMPANION DATA SETS

PREPARED BY:	Dr. Gregory S. Forbes
ACADEMIC RANK:	Associate Professor
UNIVERSITY AND DEPARTMENT:	The Pennsylvania State University Department of Meteorology
NASA/KSC	
DIVISION:	Communications and Instrumentation
BRANCH:	Instrumentation and Measurements
NASA COLLEAGUE:	Carl Lennon
DATE:	August 15, 1994
CONTRACT NUMBER:	University of Central Florida NASA-NGT-60002 Supplement: 17



## ACKNOWLEDGEMENTS

Participation in the NASA/ASEE Summer Faculty Fellowship Program has been an enjoyable and professionally stimulating experience. Appreciation is extended to all those who support this program financially, and to the many individuals who made presentations or gave tours to the Faculty Fellows. Particular thanks are extended to Dr. Loren A. Anderson, Co-Director of the NASA/ASEE Summer Faculty Fellowship Program, and to Kari L. Stiles, Administrative Assistant, who coordinated the program extremely well.

It was a great pleasure to work with Carl Lennon and others associated with the Lightning Detection and Ranging (LDAR) system in TE-CID-3. Carl Lennon is to be congratulated for the development of the LDAR system, which shows great capabilities in revealing the presence of electrical discharges within, and emanating from, thunderstorms. His support and encouragement of the applied research reported here is appreciated. The author benefitted from discussions with Launa Maier, who has vast knowledge of thunderstorms and their electrical processes.

The author is very appreciative of the efforts of the NYMA employees, Steve Schaefer and Phil Gardner, who operate the LDAR system and archive its data, and patiently dealt with many data requests and the increased computer load while the data were being processed. Steve was particularly helpful in retrieving data for the studies described below.

Many groups and individuals helped provide companion data sets for use in the study. Bart Hagemeyer (MIC), Dave Sharp (SOO) and Steve Hodanish, all of the National Weather Service Office in Melbourne, assisted in WSR-88D radar data acquisition. Phil Gemmer of EG&G and Hal Herring, Susan DeRussey and Val Valek of CSR provided field mill and wind tower (surface mesonet) data. Jim Medina (TE-CID-1) and Mike Moore (NYMA) helped acquire KSC wind profiler data. Gerry Talley of TE-CID-2 and Al Cater (LSOC) provided LLP data and roof camera video data. Greg Taylor and Mark Wheeler of the Applied Meteorology Unit (AMU; ENSCO) helped acquire Patrick AFB radar data using the McGill radar display system.

Two graduate students participated in the summer research project: Steven G. Hoffert, a graduate student in meteorology at Penn State University and Lt. Nathan E. Drummond of the Air Force Institute of Technology and the Ohio State University Department of Geography and Atmospheric Science. They assisted in cloud photography, radar data retrieval, and took the lead in obtaining and implementing radar display software and overlaying LDAR data on the radar imagery. Steve also served as liaison to the National Weather Service Office in Melbourne in their process of learning to use LDAR data in operational weather forecasting and kept track of the meteorological scenarios in which thunderstorms were developing. Their participation helped make the summer research program a success. John Madura, Chief, Weather Projects Office (TM-LLP-2), provided financial support for the participation of Steve Hoffert.

The processing of large quantities of data from diverse sources required considerable computer support. Mark Sorger and Carol Lundberg of EG&G provided exceptional service in loading data onto the KSC computer system (KSDN). John Kiriazes and Steve Tam of TE-CID-3 helped provide access to the Internet, and helped the graduate students gain access to computer workstations. Art Person of Penn State provided computer assistance via e-mail. Workstations in the Wave Analysis Lab were used to display radar data and LDAR overlays, and the assistance of Tom Henning (NGTS) is appreciated. Radar display software was written by and obtained from Dave Priegnitz, Institute of Atmospheric Sciences, South Dakota School of Mines and Technology.

The author looks forward to a continued interaction with Carl Lennon, Launa Maier, Steve Schaefer, Phil Gardner, and others using LDAR data for weather applications, including Robin Schumann (ENSCO) and Frank Merceret of the AMU. Our goal is to help the operational weather forecasters of the 45th Weather Squadron--detached out of Patrick AFB, USAF Space Command--who provide KSC with operational weather support from the Cape Canaveral Forecast Facility.

## ABSTRACT

Research was conducted to use the KSC Lightning Detection And Ranging (LDAR) system, together with companion data, in four subprojects: weather forecasting and advisory applications of LDAR, LDAR in relation to field mill readings, lightning flash and stroke detection using LDAR, and LDAR in relation to radar reflectivity patterns and KSC wind profiler vertical velocities. The research is aimed at developing rules, algorithms, and training materials that can be used by the operational weather forecasters who issue weather advisories for daily ground operations and launches by NASA and the United States Air Force.

During the summer of 1993, LDAR data was examined on an hourly basis from 14 thunderstorm days and compared to ground strike data measured by the Lightning Location and Protection (LLP) system. These data were re-examined during 1994 to identify, number, and track LDAR-detected storms continually throughout the day and avoid certain interpretation problems arising from the use of hourly files. An areal storm growth factor was incorporated into a scheme to use current mappings of LDAR-defined thunderstorms to predict future ground strikes.

During the summer of 1994, extensive sets of LDAR and companion data have been collected for 16 thunderstorm days, including a variety of meteorological situations. Detailed case studies are being conducted to relate the occurrence of LDAR to the radar structure and evolution of thunderstorms. Field mill (LPLWS) data are being examined to evaluate the complementary nature of LDAR and LPLWS data in determining the times of beginning and ending of the ground strike threat at critical sites. A computerized lightning flash and stroke discrimination algorithm has been written that can be used to help locate the points of origin of the electrical discharges, help distinguish in-cloud, cloud-ground, and upward flashes, and perhaps determine when the threat of ground strikes has ceased. Surface wind tower (mesonet), radar, sounding, and KSC wind profiler data will be used to develop schemes to help anticipate the timing and location of new thunderstorm development. Analysis of this data will continue in graduate student research projects.

## SUMMARY

Lightning Detection and Ranging (LDAR) data have been examined from thunderstorms during the summers of 1993 and 1994. The 1993 data set, consisting of 33 hours of data from 14 days, has been extensively examined to determine the locations of cloud-ground strikes relative to the areas experiencing LDAR events, which are sometimes related to ground strikes and to the more frequent in-cloud and cloud-cloud discharges. Extensive software was written to cluster the LDAR data points into LDAR-defined thunderstorms, number them, and track their movements. The locations of ground strikes detected by the KSC Lightning Location and Protection (LLP) system were then compared to the LDAR storms. Ninety-eight percent of the ground strikes occurred within the boundaries of the LDAR storms or within 2 km of their edges. The 2 km margin allows for modest position mislocations by the remote sensing systems (primarily LLP) and for tilted ground strikes whose lower portions are not typically detected by the LDAR system. For individual storms, LDAR events occur aloft, on average, 4-5 minutes before the first ground strike. Typically the first LDAR events are centered near 8 km.

An extrapolation scheme which used existing LDAR storms and their movements to predict future ground strike locations was examined. Modest success was obtained for forecasts of less than 10 minutes duration. An areal storm growth factor was also incorporated into the scheme, giving somewhat improved results in forecasts longer than 5 minutes. Beyond 10 - 20 minutes, however, the extrapolation scheme would not prove acceptable as an automated warning tool. Further analysis revealed that this type of scheme performed reasonably well once the day's thunderstorm activity was well underway. However, during the first half hour--when the number of thunderstorms is rapidly increasing--the forecast problem is one of anticipation of where new thunderstorm cells will form, rather than one of extrapolation of existing storms.

Software was written to examine and intercompare companion meteorological data sets and begin to address the problem of new thunderstorm cell development. These include LPLWS (Launch Pad Lightning Warning System--field mills), radar, KSC wind profiler, and surface mesonet (wind tower) data. Data sets have been obtained and initial case studies performed to test the software. Analyses of these data sets will continue.

LDAR has been superimposed on radar to relate the evolution of the storm lightning pattern to thunderstorm structure. Initial examples have been presented showing the location of the first LDAR events in storms with respect to radar reflectivity patterns, typically at a location just above the highest reflectivity core. The LDAR pattern at the beginning of a microburst-producing storm has been documented. The quasi-stratiform radar reflectivity pattern accompanying a broad, diffuse in-cloud flash has been shown.

Field mill readings are being examined to determine critical values of electric field at the time of beginning and end of the threat of lightning at critical sites. This relates to a forecast problem concerning the likelihood of lightning from electrified anvil or debris clouds. Examples are shown.

Software was written to identify individual flashes and strokes contained within the volume of LDAR data. This can be used to help identify isolated ground strikes from anvil using LDAR data. The points of origin of the LDAR-detected flashes and strokes can be used to help identify the three-dimensional positions of the positive and negative charge centers within thunderstorms, and can be related to radar depictions of the storm precipitation structure in these regions. Examples are shown.

The generation of training materials has also been an objective of the project. In addition to the material within this report, seminars were given to operational weather forecasters of the National Weather Service and the United States Air Force 45th Weather Squadron. Copies of the viewgraphs and slides from these presentations have been made available to these groups, to the Applied Meteorology Unit, and to the NASA Weather Projects Office.

## TABLE OF CONTENTS

<u>Section</u>	<u>Title</u>	<u>Page</u>
I	INTRODUCTION .....	7
1.1	The LDAR and LLP Systems and Data Processing .....	7
1.2	Past Results and Current Objectives .....	9
II	WEATHER FORECASTING AND ADVISORY APPLICATIONS OF LDAR .....	10
2.1	Potential Mesoscale and Synoptic Climatology Applications .....	10
2.2	LDAR Lead Times .....	10
2.3	Evolution of LDAR in Thunderstorms .....	10
2.4	Prediction of Future Ground Strikes by Extrapolation .....	12
2.5	Ground Strikes from Anvils .....	13
III	LDAR IN RELATION TO FIELD MILL READINGS .....	15
3.1	Intercomparison of LDAR, LLP, and Field Mill Readings .....	15
3.2	Case Study of Field Mill Lightning Hazard Thresholds .....	15
IV	LIGHTNING FLASH AND STROKE DETECTION USING LDAR .....	17
4.1	Lightning Flash/Stroke Identification Algorithm; Noise Identification .....	17
4.2	Thresholds for Flash and Stroke Detection .....	17
V	LDAR IN RELATION TO RADAR REFLECTIVITY PATTERNS AND KSC WIND PROFILER VERTICAL VELOCITIES .....	22
5.1	Intercomparison of LDAR to Radar .....	22
5.2	KSC Wind Profiler Vertical Velocities in Relation to a Layered LDAR Structure .....	26
VI	CONCLUDING REMARKS .....	28
	REFERENCES .....	29

## LIST OF ILLUSTRATIONS

<u>Figure</u>	<u>Title</u>	<u>Page</u>
Figure 1-1	LDAR cubes superimposed on LDAR data points used in LDAR storm classification .....	8
Figure 2-1	Frequency of lightning occurrence based on 1993 LDAR sample ..	11
Figure 2-2	Hypothetical limits to accuracy of extrapolation forecasts of lightning ground strikes .....	14
Figure 3-1	Field mill readings as a function of time in relation to the distances to the nearest LDAR and LLP lightning events ...	16
Figure 4-1	Perspective view of all LDAR data points during minute 0106 UTC of day 154, 3 June 1993 .....	18
Figure 4-2	Perspective view of flash 2 .....	19
Figure 4-3	Perspective view of flash 4 .....	20
Figure 5-1	South-north cross-section of thunderstorm with LDAR overlay, from 1948 UTC on day 210, 29 July 1994 .....	23
Figure 5-2	Constant-altitude display of radar reflectivities with LDAR overlay at 7 km from 1958 UTC on day 210, 29 July 1994 ..	24
Figure 5-3	Constant-altitude display of radar reflectivities with LDAR overlay at 6 km from 2153 UTC on day 210, 29 July 1994 at 6.0 km .....	25
Figure 5-4	Time-height section of LDAR events over the KSC wind profiler site in relation to patterns of updraft and downdraft .....	27

## I. INTRODUCTION

The Kennedy Space Center (KSC) is located in one of the regions of the United States (and even the world) that encounters the most lightning strikes to ground per unit area (refs. 1,2,3). The possibility of lightning at the surface or aloft is, of course, a hazard that must be avoided during launches. On a daily basis, however, there are many operations at KSC which must be curtailed if there is a threat of a lightning strike to ground in the vicinity. The accuracy and timeliness of lightning advisories, therefore, has both safety and economic implications. The ultimate goal of the research described in this report is to provide information that can be used to improve the process of real-time detection and warning of lightning by weather forecasters who issue lightning advisories.

Special networks of remote sensing equipment have been established to provide highly accurate information concerning lightning in the vicinity of KSC: the Lightning Location and Protection (LLP) system, the Lightning Detection and Ranging (LDAR) system, and a Launch Pad Lightning Warning System (LPLWS). In addition, a Catenary Wire Lightning Instrumentation System (CWLIS) detects electrical surges in wires at the launch pads when struck by lightning. The first two systems detect lightning signatures. LPLWS, by contrast, responds not only to lightning but also detects electric fields at the surface induced by electrified clouds, thunderstorms, and other atmospheric conditions. Data from the LLP, LPLWS, and LDAR systems were used in this study.

### 1.1 THE LDAR AND LLP SYSTEMS AND DATA PROCESSING

The LLP system (ref 4) detects lightning ground strikes through use of a network of magnetic direction finding antennae which sense electromagnetic disturbances triggered by lightning in a broad band of frequencies. Individual antennae detect a particular ground strike at different azimuth angles, and the location of the ground strike is essentially determined by finding the point of intersection of lines drawn from the antennae toward the source of the disturbance. The LLP system is approximately 90% efficient in detecting ground strikes near KSC, with position accuracy of about 1 km.

The LDAR system was developed by Carl Lennon and colleagues at KSC TE-CID-3 (ref 5). Its antennae detect lightning-induced disturbances at 66 MHz (VHF) frequency. This system uses a time of arrival (TOA) approach, and achieves extremely accurate timing through use of the Global Positioning System (GPS). The lightning-induced disturbance, travelling at the speed of electromagnetic propagation, arrives at different antennae at slightly different times. The three-dimensional position of the lightning source is determined by essentially converting these time offsets into distance differences, and then performing a triangulation. The LDAR system began real-time operation in June, 1992.

The LDAR system can generate up to 10,000 data points per second, yielding numerous data points per lightning flash. Tests of the position accuracy of the LDAR data by Launa Maier have shown that within 10 km of the central antenna, 95% of the data points are accurate to better than 200m, and 50% are accurate to better than 100m. Dots on Figure 1-1 illustrate a sample plot of LDAR data points (events) during one minute, projected to their positions at the surface. Raw LDAR data points are represented by a time and by x, y, and z positions relative to the LDAR central site. Some of the studies during 1994 used raw LDAR data.

Also shown in Fig. 1-1 is a squared-off portrayal of the area experiencing LDAR events. The squares represent post-processed LDAR data used in other facets of this research. LDAR data were composited into a four-dimensional array, consisting of the number of LDAR events within a minute and a volume. During 1993 (ref. 6) the volume was a cube having sides of length 1 km. Array elements extended from 52 km west of the LDAR central site to 52 km east, from 40 km south to 40 km north, and from 0 to 20 km in elevation. During 1994, the volumes used were rectangular wafers 1 km<sup>2</sup> in cross-section and covering the same domain, but 0.25 km in vertical thickness, extending from 0 to 22 km.

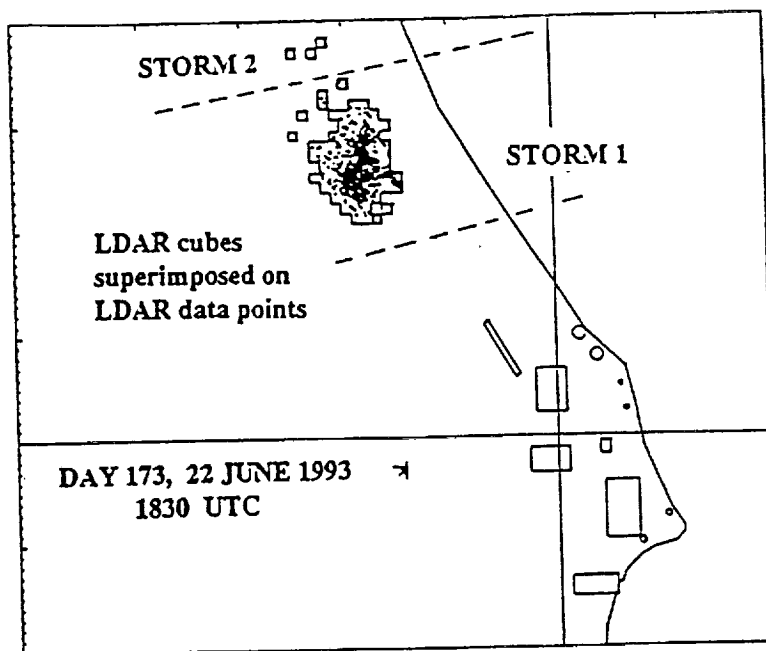


Figure 1-1. LDAR cubes superimposed on LDAR data points used in LDAR storm classification. Only a portion of the -52:52 by -40:40 km domain is shown.

Contiguous and adjacent LDAR volumes were then clustered together to form LDAR-defined storms. LDAR volumes separated by more than 3 km from a neighbor become part of a separate storm, as depicted in Fig. 1-1. Additional software examines the classified storms, discards as spurious data any storms occupying less than 4 km<sup>3</sup>, and numbers storms consistently from minute to minute. During 1993, data files were one hour in duration, such that storm number continuity could be lost between successive hours. Software has now been implemented to number storms consistently throughout a multi-hour case.

The storm numbering process uses the LDAR event-density-weighted mean horizontal position of the LDAR storm center or "centroid" and its variations with time. In this procedure, certain time and distance limits are empirically invoked to deal with numbering of intermittent LDAR storms and storms that split or merge. LDAR storms are assigned a new number if their centroid does not fall within 6 km of the position of an existing storm from an earlier time. Thus, a storm resulting from a merger of two storms could be assigned either one of the existing storm numbers--in the case of a large storm "absorbing" a smaller one--or be assigned a new number--if the composite centroid was more than 6 km from either of those of the previous storms. In the case of intermittent storms, a 10-minute preceding period is searched. Storm area, depth, volume, LDAR event density, and other parameters are monitored with time. Algorithms have been written to track LDAR-defined storms through examination of the rates of change of their centroid positions. Additional details can be found in Reference 6.

## 1.2 PAST RESULTS AND CURRENT OBJECTIVES

This was the second summer of study involving research to utilize lightning detection and ranging (LDAR) data, together with companion data sets, aimed at developing rules, algorithms, and training materials that can be used by the operational weather forecasters who issue weather advisories for daily ground operations and launches by NASA and the United States Air Force. Research during 1993 enabled the development of a computerized scheme for clustering the LDAR data into groups of data points associated with individual thunderstorms (as described above), tracking these LDAR-defined storms, and comparing the positions of the LDAR-detected lightning to those of other remote sensing systems. It was determined that LDAR-detected discharges aloft within the storm precede ground strikes by about 5 minutes in the region within 60 km of KSC, making LDAR a very useful tool for issuing very-short-term weather advisories and warnings. By recognizing and including storm movement in a forecast scheme, mappings of current LDAR data points can be used to make forecasts of future cloud-ground strikes.

Research during 1993 showed, however, that beyond about 10 minutes areal storm growth and the development of new thunderstorm cells became increasingly important factors in the prediction of future lightning ground strikes. Hence, the focus of the 1994 research was to include a storm growth factor in the forecast scheme, and to begin to examine companion meteorological data sets that could ultimately be used in forecast schemes to help the forecasters anticipate new thunderstorm formation. In addition, forecasters must determine when the lightning threat at a site has ended--a task made difficult because electrified anvil clouds are often left behind above a site long after the core of the storm has exited the region. Thus, work was begun to examine this problem.

Research summarized in this report was conducted in parallel as four subprojects: (1) weather forecasting and advisory applications of LDAR, (2) LDAR in relation to field mill readings, (3) lightning flash and stroke detection using LDAR, and (4) LDAR in relation to radar reflectivity patterns and KSC wind profiler vertical velocities. Each of these subprojects is summarized briefly below.

## II. WEATHER FORECASTING AND ADVISORY APPLICATIONS OF LDAR

### 2.1 POTENTIAL MESOSCALE AND SYNOPTIC CLIMATOLOGY APPLICATIONS

Figure 2-1 shows a mapping of the frequencies of occurrence of LDAR events above the -52:52 by -40:40 km domain during the 1993 sample, consisting of 33 hours of LDAR data from 13 days in June and July and mainly between the hours of 1500 and 2100 UTC. Numbers represent the percentage of time (minutes) with LDAR data above each 1 km<sup>2</sup> area of the domain. Dramatic gradients in frequency, such as the couplet 15-25 km west of KSC, suggest the meso-gamma-scale importance of river breeze circulations and land-water distributions on summer thunderstorm formation in this area. While the detail in the pattern in this limited sample is undoubtedly impacted by individual cases, the overall pattern nevertheless is indicative of a general tendency for cells to develop more frequently over regions west of KSC. It is also known (e.g., ref 7) that the timing and pattern of thunderstorm development is strongly a function of the prevailing wind direction. Sounding data has been collected, and will be used together with surface, radar, and other data in studies aimed at improving prediction of thunderstorm formation.

### 2.2 LDAR LEAD TIMES

The lead time between first appearance of LDAR events in a storm and first ground strike was computed in several ways. In the 1993 study, 27 storms were examined that occurred during the first hour of the day when storms were in the domain. The average lead time was 5.26 minutes, and 11% of the storms had ground strikes during the first minute of LDAR event existence.

Once storms were renumbered consistently throughout the case (rather than independently by hour) in 1994, all hours were used to recompute lead time, resulting in a larger sample and one typical of all new storm formations. To avoid storms already in existence and moving into the domain, only LDAR storms with centroids in a smaller domain were used: -48:48 by -36:36. In addition, storms "newly formed" by the objective scheme as a result of merging or splitting cells were eliminated by ignoring new storms forming within 6 km of pre-existing LDAR storms. For the 88 storms defined in this manner, the mean lead time was 4.01 minutes, with 28% of the storms producing ground strikes during the first minute of LDAR activity. Lead times in the sample ranged from 0 to 20 minutes.

It should be pointed out that from a forecaster's perspective the 4-5 minute lead times cited here pertain to the relatively uncommon situation in which thunderstorms develop directly above a forecast site. Thus, LDAR more typically provides a longer lead time by pointing out that thunderstorms are developing within the region and may soon pose a threat to a forecast site.

### 2.3 EVOLUTION OF LDAR IN THUNDERSTORMS

LDAR storms in the renumbered 1993 sample were examined to identify common features of LDAR pattern evolution. Starting with the 88 storms forming within the network, as described above, the sample size was reduced to 59 by elimination of short-lived storms (duration less than 6 minutes). Of the remaining storms, the mean duration was 25 minutes, with one storm lasting 94 minutes. This is a reasonable value for individual thunderstorms, and the objective numbering scheme tends to exclude broad, long-lived mesoscale storm systems formed through mergers.

A noticeable aspect of the LDAR storm evolution was that the early and late stages of their existence tended to be episodic. Gaps of several minutes between flashes were typical within the 5 minutes following the first minute of LDAR activity, and again during the last 10 minutes.

LDAR events first occurred near 8 km in most storms. The mean height of the center of storms' first LDAR events was 7.9 km, with no center below 3.25 km or above 11.25 km. Seventy-four percent of the centers developed between 7.25 and 9.75 km. These altitudes suggest the importance of an in-cloud temperature of

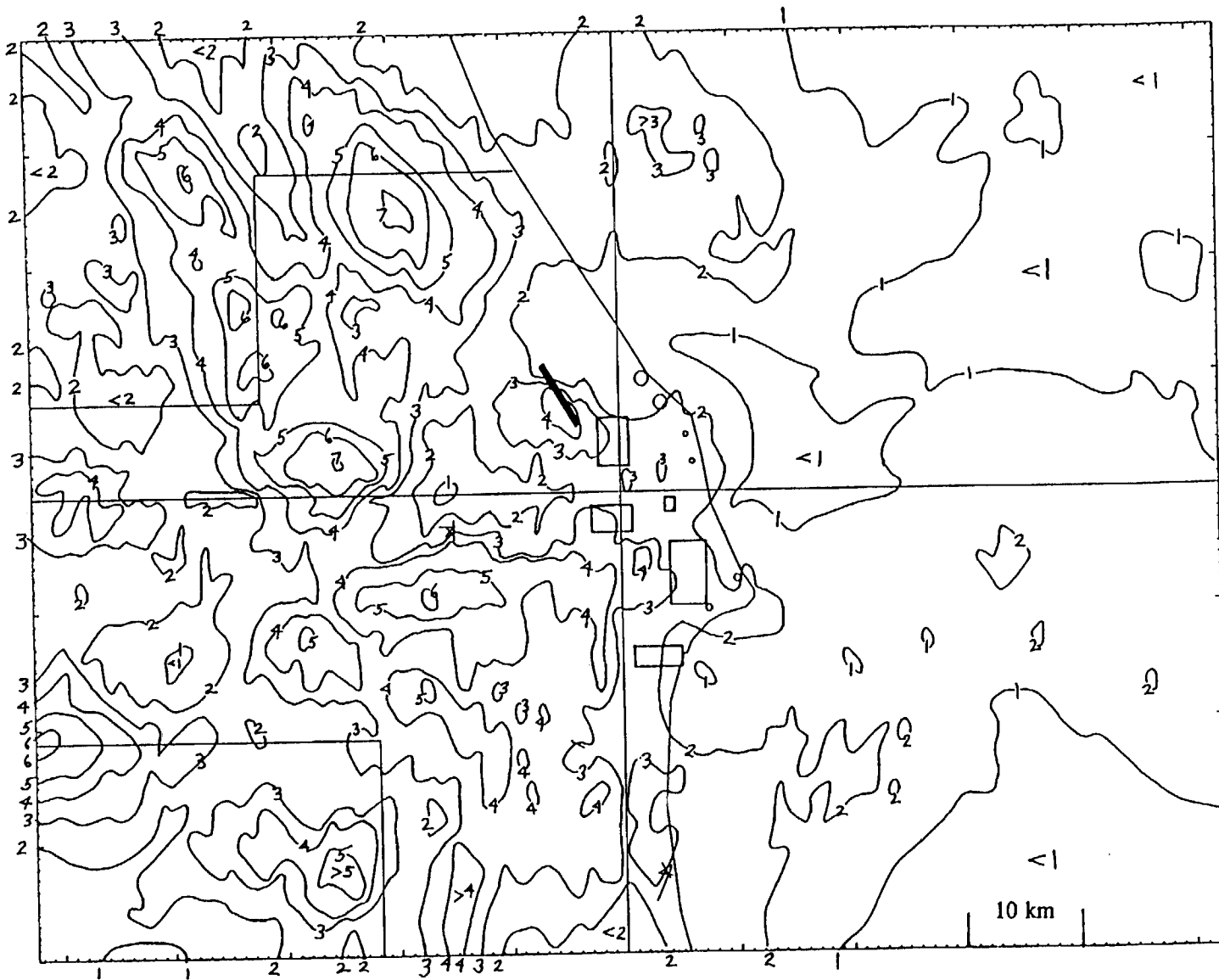


Figure 2-1. Frequency of lightning occurrence per square kilometer per minute, using LDAR data from the 1993 sample: 33 hours on 13 days. Numbers are in percent.

-15 to -20 °C, at which mixed-phase precipitation and electrification processes are likely.

The individual LDAR storm tended to grow vertically and horizontally rather rapidly, expanding its areal cross-section by a factor of 3 during the first 10 minutes, a total factor of 5 by 20 minutes, and a total factor of 10 by about 60 minutes. No distinct trend was seen in the limited number of storms with longer durations. It should be pointed out that mesoscale convective events can last much longer, and grow much larger, due to the development of mesoscale clusterings of cells into squall lines or mesoscale convective systems and known to contain mesoscale circulations different from those of individual thunderstorms. Such merger processes typically result in assignment of new storm numbers via the objective numbering scheme. Thus, those mesoscale phenomena have been excluded from the composites.

#### 2.4 PREDICTION OF FUTURE GROUND STRIKES BY EXTRAPOLATION OF LDAR STORMS

Based upon the 1993 sample, within the concurrent minute, 85% of the LLP-measured ground strikes fell inside the bounds of the LDAR-defined storms and 98% inside or within 2 km of the edge. The latter 2 km strip allows for (1) tilted flashes not detected at low levels by LDAR and (2) location inaccuracies largely attributed to LLP positioning. LDAR event rates decline markedly below 3 km, at least partly due to the increased importance of return strokes at these levels which--due to their more continuous rather than pulsed emission characteristics--are not amenable to detection by LDAR.

An extrapolation scheme was developed in 1993 to determine the percentage of future ground strikes that could be successfully predicted by extrapolating existing LDAR patterns with storm motion vectors. It was determined that by a forecast time of about 15 minutes, half of the future ground strikes would be missed, due to a combination of existing storm growth and new storm formation.

During 1994 an additional factor was added to the extrapolation scheme, allowing expansion (or occasional contraction) of storm area by extrapolation of the storms' growth rate histories. The historical record was chosen to be equal in time to the desired forecast period, or as long as possible if the storm was not that old. Growth rates were computed and applied based upon the rate of change of the width of the LDAR storms in the x and y directions, expressed as percentage changes relative to the start time size.

Table 2-1 shows the results of the augmented extrapolation scheme. Incorporation of an areal expansion factor increased the percentage of ground strikes falling within the bounds of the LDAR storm at all forecast times. The growth factor had no effect on the percentage of ground strikes within 2 km of storm edge for forecasts of durations to 5 minutes, and yielded only modest improvements at longer forecast intervals. The main conclusion is that anticipation of non-systematic growth, and particularly development of new thunderstorm cells, becomes critical in making forecasts for duration longer than 15 minutes.

Further examination of the issue of ground strike predictability via extrapolation of LDAR gave a bit more room for optimism and shed light on the nature of the prediction problem. Figure 2-2 shows the practical limits on predictive skill via extrapolation schemes as a function of time during the convective episode. Here an episode begins at the time of first LDAR occurrence within the -52:52 by -40:40 km domain, rather than being linked to an individual storm. To develop the graphs, it was hypothesized that a perfect prediction could be made of the future positions and sizes of LDAR storms, such that only new thunderstorm formation was not accounted for. Of course, this is more easily assumed than achieved.

The inference to be drawn from Fig. 2-2 is that the worst forecast problems tend to come early in the convective portion of the day, particularly during the first half hour when relatively few storms are already in existence and new ones are forming frequently. After about the first 90 minutes of the convective period,

sufficient numbers of storms are in existence that their extrapolation can lead to increased success rates, but perhaps never to a point of acceptability in a 20-30 minute forecast.

TABLE 2-1

**PREDICTION OF FUTURE CG STRIKES BASED UPON  
EXTRAPOLATION OF EXISTING LDAR STORMS,  
WITH AND WITHOUT CONSIDERATION OF  
GROWTH/DECAY FACTOR OR AGE OF EPISODE**

% OF LLP EVENTS FALLING WITHIN PREDICTED AREA

FORECAST TIME	NO GROWTH FACTOR		RECENT GROWTH EXTRAPOLATED	
	INSIDE EDGE	WITHIN 2 km	INSIDE EDGE	WITHIN 2 km
3 min	71	88	80	87
5	64	84	74	83
10	44	67	61	72
15	31	50	49	59
20	20	35	39	48
30			23	31

## 2.5 GROUND STRIKES FROM ANVILS

There is great interest in knowing when and if ground strikes emanate from thunderstorm anvils, since they frequently persist over a forecast site long after the convective tower portion of the thunderstorm has passed. A preliminary study was conducted using LDAR and LLP data to determine the frequency of ground strikes from anvils. This study was done by defining an altitude corresponding to an anvil base, and then defining LDAR anvil areas as those having no LDAR events at lower elevations. However, this method excludes from consideration not only the cases where the lower LDAR events emanate from in-cloud lightning, but also excludes the cases of ground strikes from anvil detected by LDAR (thus, yielding LDAR data points at sub-anvil levels). Thus, this task was postponed until an LDAR flash detector could be developed to identify the latter situations. This project is described in section IV.

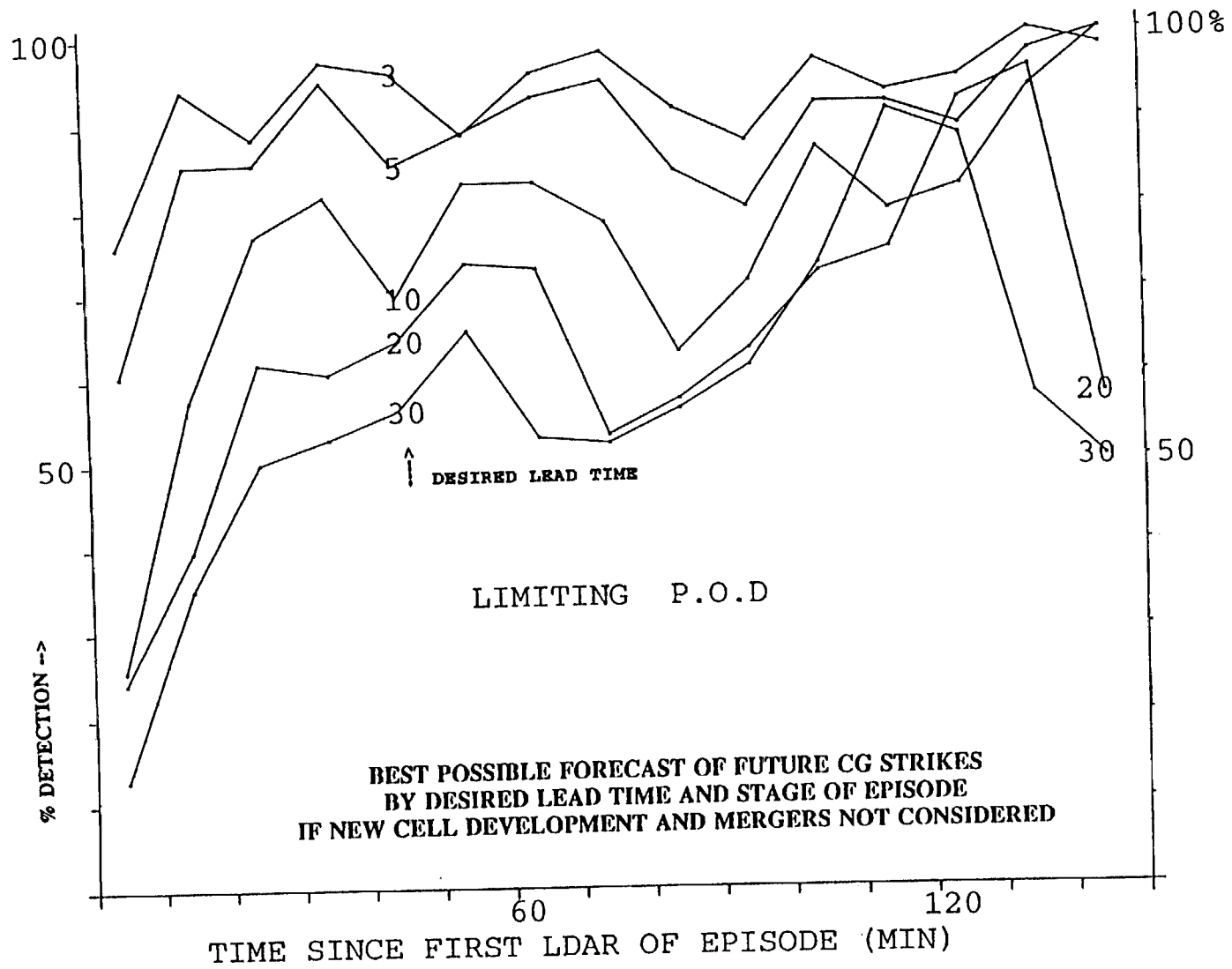


Figure 2-2. Hypothetical limits to accuracy of extrapolation forecasts of lightning ground strikes as a function of time since the first LDAR event in the domain and forecast duration.

### III. LDAR IN RELATION TO FIELD MILL READINGS

#### 3.1 INTERCOMPARISON OF LDAR, LLP, AND FIELD MILL READINGS

Vertical electric fields at the surface are measured by an "old" and a new, upgraded network of electric field mills deployed over KSC and surroundings. The lower portion of Figure 3-1 shows a time series of electric field readings. These values are from old mill 20, just northeast of the LDAR central site. Readings become increasingly negative as the negative charge center builds within overhead or nearby thunderstorms, as shown through 2015 UTC. A positive surface electric field can exist beneath the lower positive charge center that sometimes develops near cloud base in heavy rain areas, and at distances beyond about 10 km from the thunderstorm where the surface electric field is dominated by the upper positive charge center within the thunderstorm anvil, as shown after about 2115 UTC. The value of the surface electric field is, therefore, a function of the magnitudes and elevations of the charge centers in nearby thunderstorms and their distances from the site. The presence of screening layers and spatial and temporal variations of atmospheric conductivity are further complicating factors (see ref 8 for a review). Dramatic, nearly discontinuous changes in electric field associated with lightning strokes and flashes are also registered in the electric field readings, such as the spike near 2049 UTC.

Shown in the upper segments of Fig. 3-1 are plots of the horizontal distances from the field mill site to the nearest LDAR and LLP lightning discharge events as a function of time (one value per minute). In this situation a thunderstorm was located west of KSC and heading southward, and its ground strikes remained 9.25 km (5 n.mi.) or more distant from the site. Several flashes aloft were recorded directly overhead by LDAR, however, resulting in spikes within the field mill trace. In the figure, small squares at 15 km indicate that the nearest event was at a distance of more than 15 km, whereas the absence of a data point indicates no events within the -52:52 by -40:40 km domain during the minute.

#### 3.2 CASE STUDY OF FIELD MILL LIGHTNING HAZARD THRESHOLDS

The main emphasis of these intercomparison studies, which are ongoing, is to determine the threshold field mill values typically associated with the beginning and end times of heightened ground strike threat at a site, and triggered lightning threat to a launched vehicle. In a case study from 21 June 1994, Julian day 172, the average field mill reading was -1958 kV/m at the time when LDAR events first came within 9.25 km (5 n.mi.) of a site, and -1237 kV/m at the time when LDAR events last were detected within that distance. A reading of more than +/- 1 kV/m is currently used as an indicator of lightning threat.

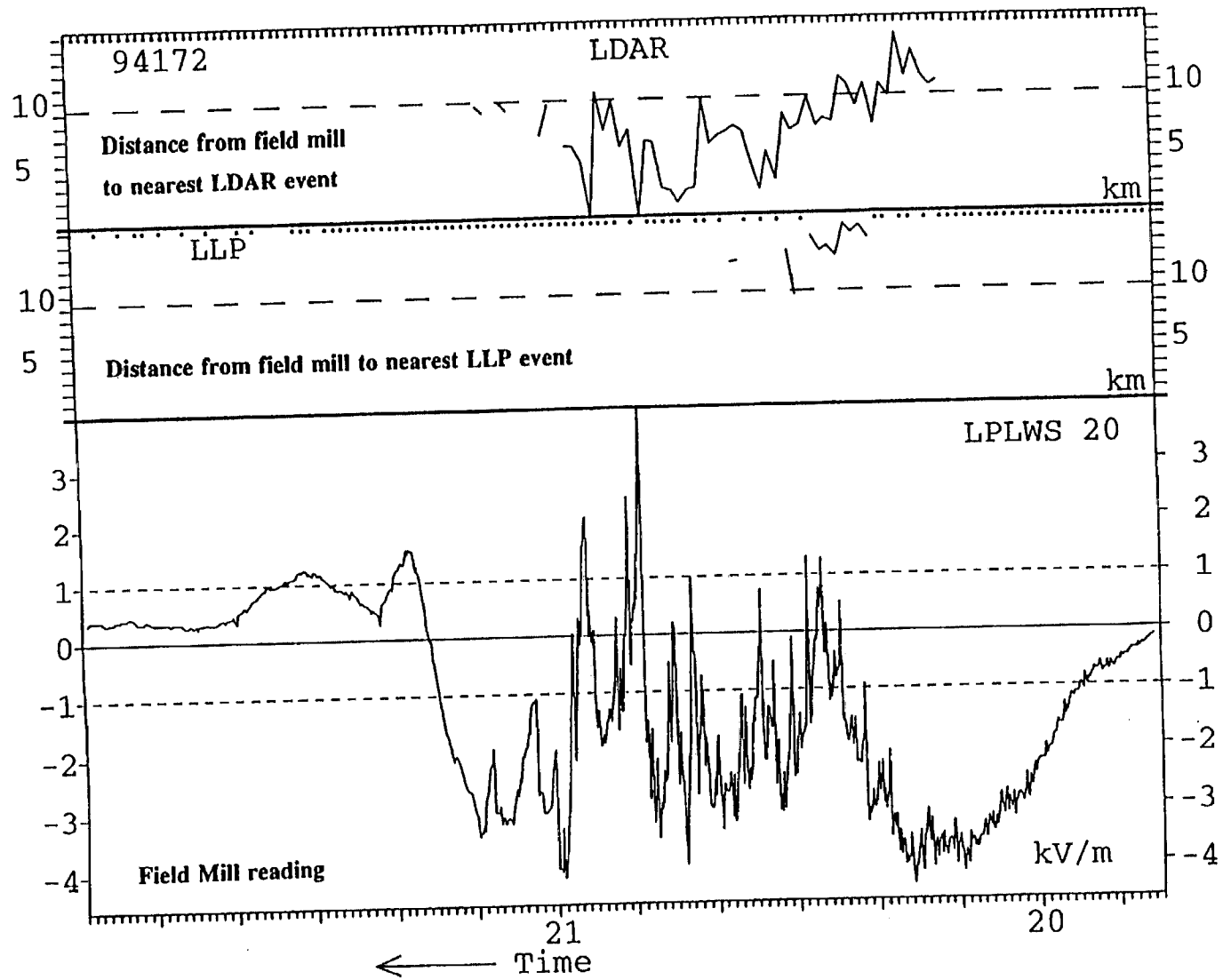


Figure 3-1. Field mill readings as a function of time for site 20 on 21 June 1994, day 172, from 1945 to 2159 UTC, in relation to the distances to the nearest LDAR and LLP lightning events.

#### IV. LIGHTNING FLASH AND STROKE DETECTION USING LDAR

##### 4.1 LIGHTNING FLASH/STROKE IDENTIFICATION ALGORITHM; NOISE IDENTIFICATION

LDAR data are recorded sequentially in time, but more than one lightning stroke and flash can be in progress and detected essentially simultaneously, from separate storms and even from within the same storm. A computerized scheme was developed to separate a file of LDAR data events into numbered groupings of data points associated with distinct flashes (or strokes; for a distinction, see discussion below). Data points falling within specified time and distance limits are classified as a distinct flash (or stroke).

The algorithm looks at each LDAR data point in the file, beginning with the first data point (record 1), which is assigned as part of flash 1. The algorithm then performs a four-dimensional "buddy" search, forward in time throughout the specified threshold interval. All future data points are assigned (numbered) as part of the same flash if they fall within the time and distance separation thresholds. The algorithm then goes on to deal with the next data point (record 2). If it is initially numbered, then all unnumbered buddies found in the forward search are assigned its number. If the data point is initially unnumbered, then it is assigned the number of the first numbered buddy found. If no buddies are found within the time and distance thresholds, then the data point is defined as part of a new flash and assigned the next unused flash number. Numbered buddy data points at forward times never are reassigned a different flash number. The algorithm continues with the third and all subsequent records until each data point in the file has been assigned a number. Additional options then permit a renumbering to separate major flashes (affiliated with more than a specified number of LDAR events), minor flashes, and noise (one-event "flashes").

The distinction between a flash and a stroke is somewhat imprecise, but the term flash is typically used to represent a time integral of about one-half second, comparable to the image of lightning seen by the human eye or in a photograph. In reality such a lightning flash is composed of a branching stepped leader, one or more return strokes, and often a dart leader. Since LDAR does not normally detect return strokes, the "strokes" cited in this research take on a somewhat different meaning.

Figures 4-1, 4-2, and 4-3 illustrate the implementation of the flash identification algorithm during one interesting minute in which a readily identifiable in-cloud flash passed over KSC. Fig. 4-1 maps all the LDAR data points during the minute 0106 UTC on day 154 of 1993. Figure 4-2 shows the data points clustered into a flash identified as number 2 (of 5 during the minute) by the algorithm when thresholds are set at 400 msec and 4.0 km. The flash consists of 737 LDAR data points.

##### 4.2 THRESHOLDS FOR FLASH AND STROKE DETECTION

A detailed human inspection of the sequence of data points comprising flash 2 of Fig. 4-2 reveals that this flash was comprised of several distinct branches or strokes, of which three were major. The first of these began just south of KSC and headed to the northwest, to near the northernmost point of the flash. Just before the first stroke terminated to the north, another major stroke began near KSC and eventually reached the most northwestern point of the flash. These strokes were primarily horizontal or upward. While the second major stroke was halfway to its western termination, the third major stroke began south of KSC and headed south and west, reaching the most southwestern point of the flash. Several smaller strokes were also identified in the region south-southwest of KSC. The use of 100 msec and 2.0 km thresholds resulted in two of the smaller strokes being identified as separate entities, as indicated in the figure, with a loss of 57 LDAR events. The use of 50 msec and 2.0 km thresholds divided this flash (and the several other flashes subjected to painstaking human inspection) into its distinct "strokes".

222

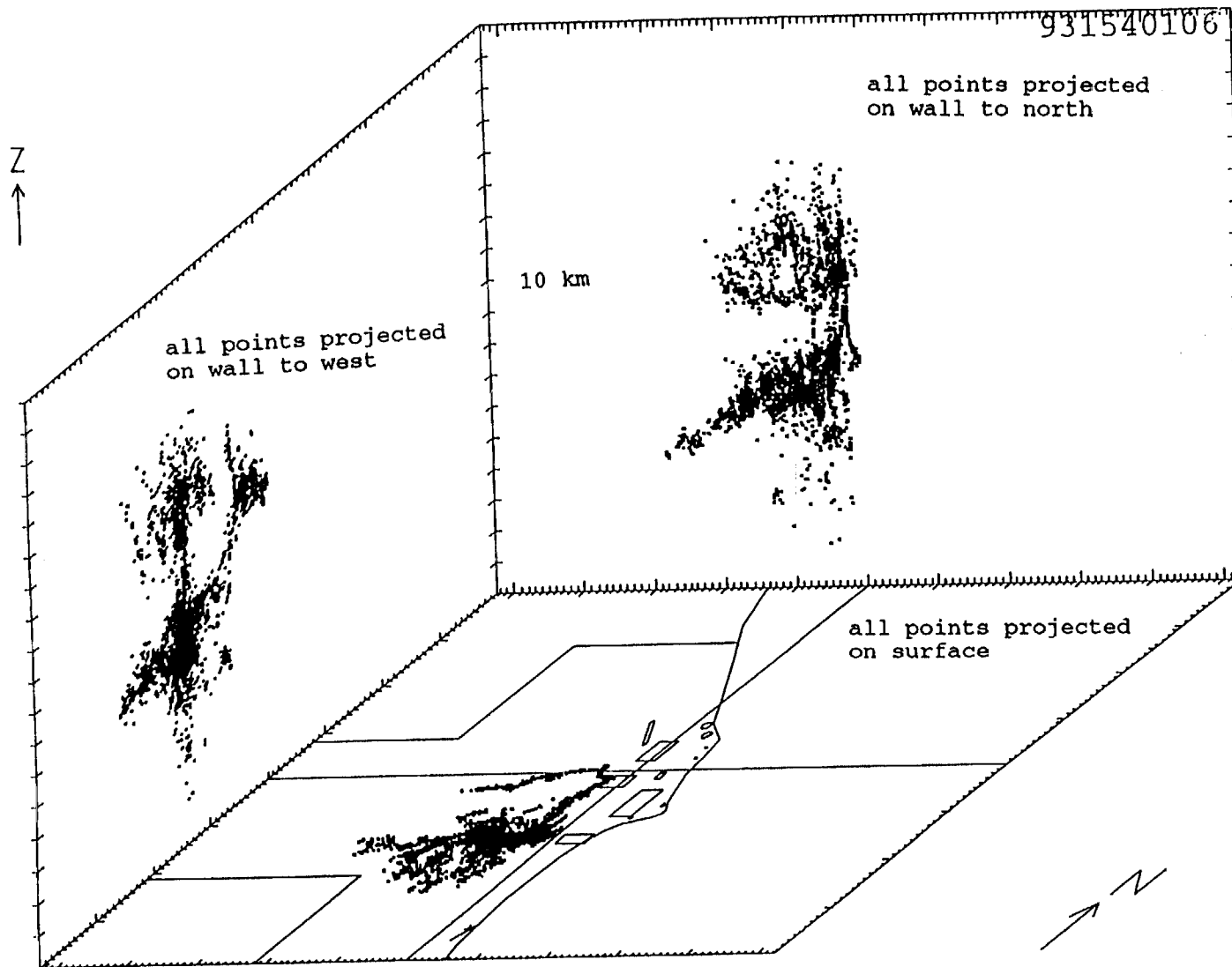


Figure 4-1. Perspective view of all LDAR data points during minute 0106 UTC of day 154, 3 June 1993.

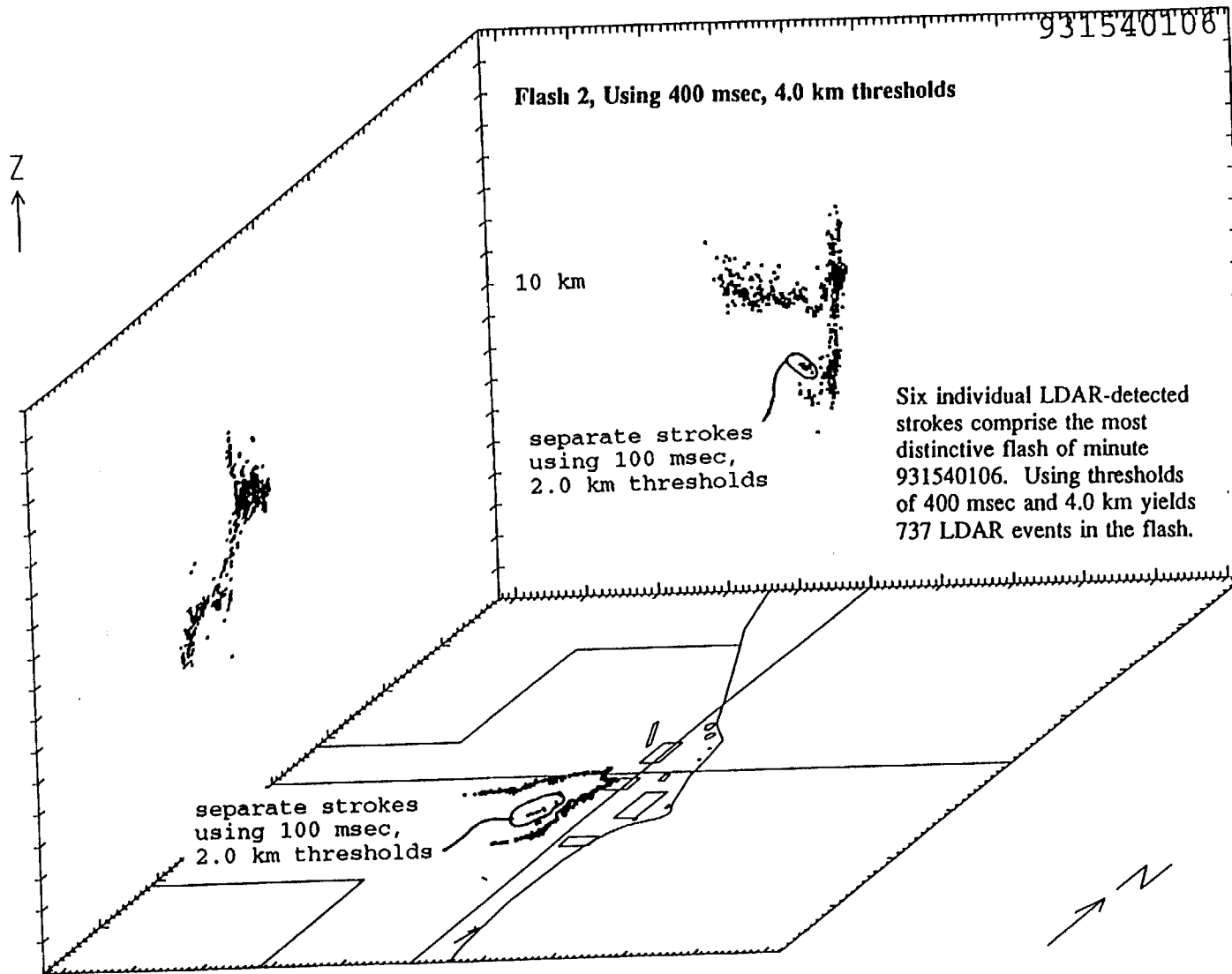


Figure 4-2. Perspective view of flash 2 out of 5 major flashes within the events of Fig. 4-1, using 400 msec and 4.0 km thresholds. These thresholds yield one major flash of duration 933 msec and consisting of 737 LDAR events. Reanalysis of Fig. 4-1 using 100 msec and 2.0 km thresholds separates this flash into two flashes, losing the 57 LDAR events as annotated.

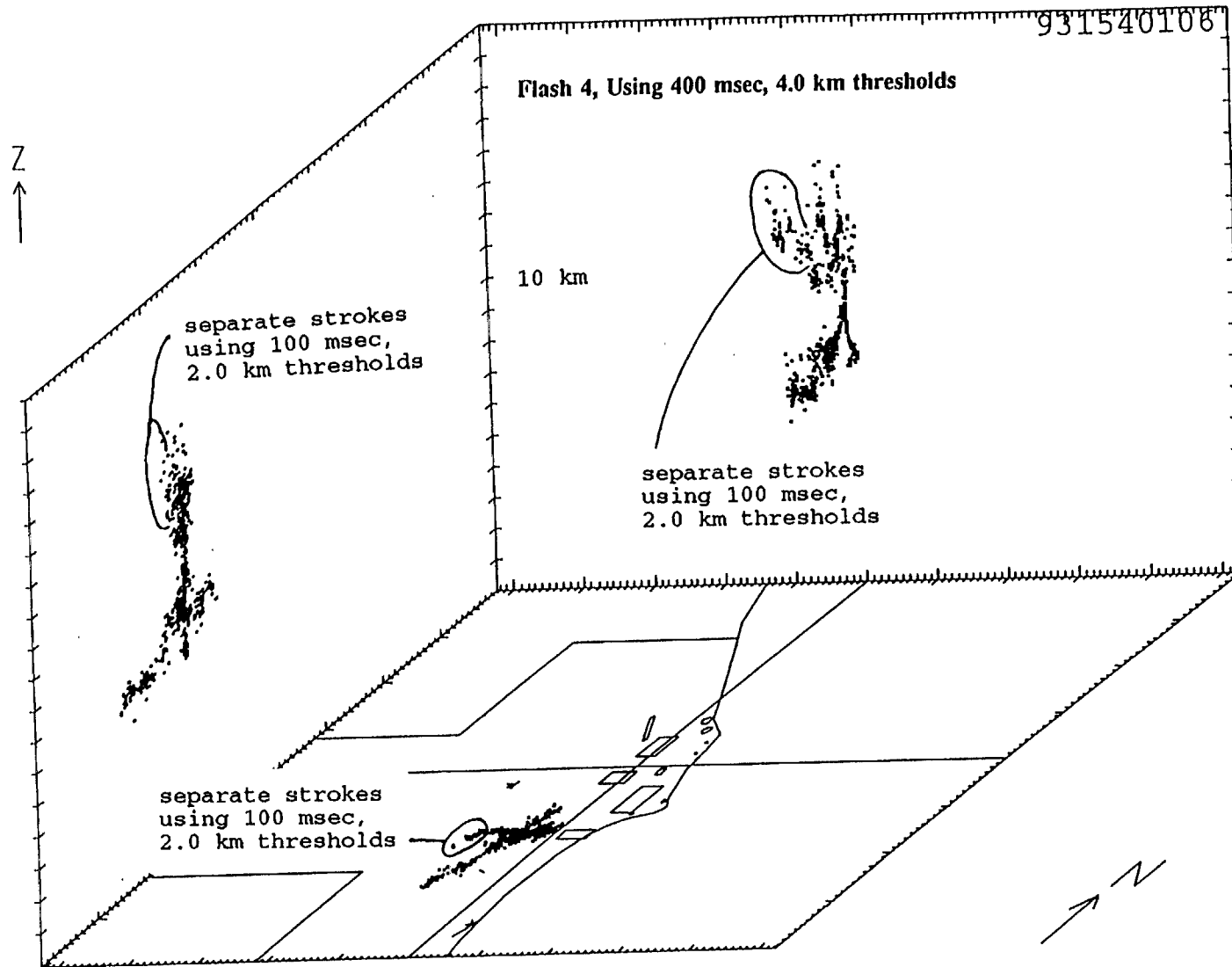


Figure 4-3. Perspective view of flash 4 out of 5 major flashes within the events of Fig. 4-1, using 400 msec and 4.0 km thresholds. Use of 100 msec and 2.0 km thresholds separates this flash into two flashes, as depicted.

Figure 4-3 shows one of the other flashes (number 4 of 5 during the minute), with thresholds of 400 msec and 4.0 km. When 100 msec and 2.0 km thresholds are used, the flash is divided into two flashes, numbers 25 and 26 of the minute, as depicted. Use of 50 msec and 2.0 km thresholds would further subdivide the flash into strokes, several of which are readily discernible in the figure.

Motivation for development of the flash identification algorithm arose during the course of several of the subtasks researched above. One is a need to isolate flashes from anvil to ground from mid-level, in-cloud flashes in order to improve understanding of the occurrence of ground strikes from anvils using LDAR. Time did not permit a return to this task after the algorithm was developed, but it will be pursued in the future.

Another motivation was the question by the author of whether there might be a variation within thunderstorms of the number and ratio of major and minor flashes, and whether this might be of value to forecasters in determining the relative likelihood of ground strikes from a storm, within different portions of the same storm, or as a function of time during the storm. In practice, the number of minor flashes depends upon what threshold is set on the minimum number of LDAR events within the flash and upon the time and distance thresholds which, when set small, tend to break major flashes into more numerous strokes. With 400 msec and 4.0 km thresholds, about 10% of the events in the small sample studied to date are classified as within minor flashes. In some minutes the minor flashes are more prevalent. Additional study is needed.

## V. LDAR IN RELATION TO RADAR REFLECTIVITY PATTERNS AND KSC WIND PROFILER VERTICAL VELOCITIES

### 5.1 INTERCOMPARISON OF LDAR TO RADAR

Because the development of lightning is affiliated with the microphysics and storm-scale dynamics of the precipitation formation process, radar--which detects the location and approximate precipitation rates within stratiform and convective storms--is a tool fundamental to lightning forecasting. Radar data from the McGill radar at Patrick AFB and the NWS Doppler weather radar (WSR-88D) at Melbourne, FL are being used in conjunction with LDAR and other companion data to examine storm structural and electrical evolution on an ongoing case study basis.

In studies performed thus far, hardcopies of radar cross-sections of storms were obtained, and software was written to overlay LDAR data onto the sections. Raw LDAR data points have been plotted in the section for the same volume sampled by the radar, namely a strip 1.85 km (1.0 n.mi.) wide. Because the radar cross-section is interpolated from a sequence of scans at progressively increasing elevation angles, it represents a reflectivity composite over a 5-minute interval. LDAR data are overlaid from a single minute near the end of the composite period, such there could be a small mismatch at lower elevations.

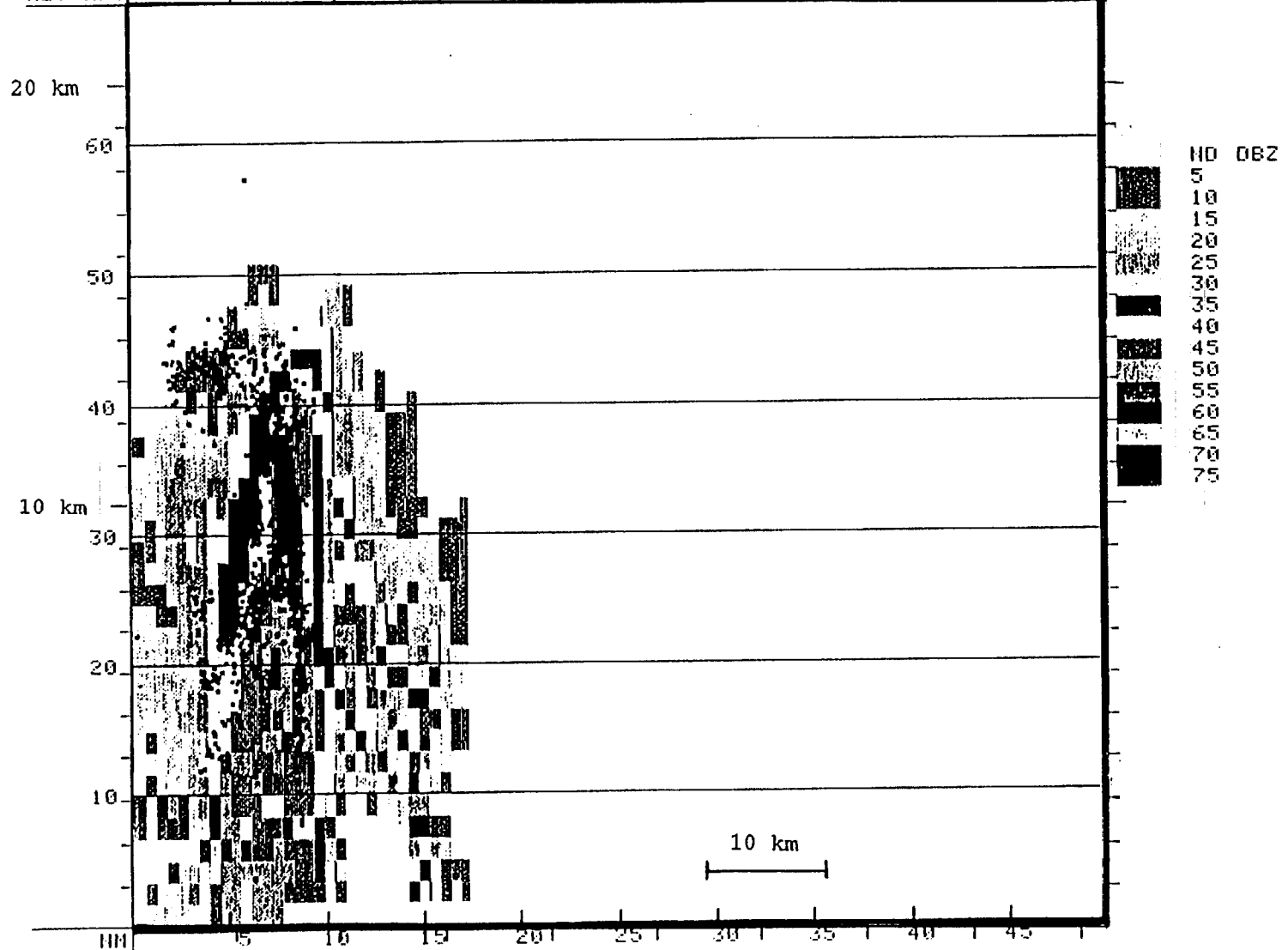
Figure 5-1 shows an example of such a cross-sectional overlay, though the color does not reproduce well in black and white. It is from a mature thunderstorm at 1948 UTC on day 210, 29 July 1994. A core of 50-57 dBZ reflectivity, indicative of heavy precipitation, is suspended aloft in the layer between 4 and 9 km (13 - 29 kft) near the center of the radar echo pattern associated with the storm. The radar reflectivity pattern with the anvil is partially truncated at the left edge of the diagram, where the radar tilt sequence does not reach elevation angle sufficiently near vertical to detect storm top.

Also shown in Fig. 5-1, a vertical column of LDAR data points extends upward from near the top of the reflectivity core at 8 km to about 13 km (42 kft), where the LDAR pattern begins to flatten into a more horizontal layer affiliated with the storm anvil. It seems likely that the LDAR column between 8 and 13 km represents in-cloud flashes between the negative and positive charge centers of the thunderstorm. The location of the negative charge center just above the core of heaviest reflectivity would be consistent with its affiliation with the mixed phase (ice and supercooled water) precipitation region of the storm, containing large drops and possibly graupel. Below 4 km at least two strings of LDAR points reveal cloud-ground strokes within and along the gradients just outside of the heavy precipitation core.

Graduate student Nathan Drummond obtained color radar display software via the Internet from Dave Priegnitz of the South Dakota School of Mines and Technology and implemented it onto workstations in the Wave Analysis Lab of TE-CID-3. Nathan and graduate student Steve Hoffert obtained archived Doppler radar data from the WSR-88D at Melbourne for several cases and Hoffert converted LDAR data to a form that could be overlaid on horizontal radar displays. Because raw LDAR data plots would often obscure much of the details of the radar display, only one LDAR data point per square kilometer is superimposed. An LDAR point was plotted if there were any LDAR data points within the square kilometer column of depth 0.75 km centered on the radar display altitude.

Figure 5-2 shows an example of a radar image with LDAR overlay, from 1958 UTC on day 210, 29 July 1994 at 7.0 km. This depicts the first LDAR events associated with a thunderstorm that produced a microburst--a strong small-scale downdraft and near-surface outflow--which caused damage on Merritt Island about 25 minutes later. The LDAR events at this time are centered just above and slightly downwind (to the north-northeast) of the reflectivity core. A younger cell just west of the microburst storm has not yet produced any LDAR events. Elsewhere on the figure, LDAR events are associated with moderate and heavy precipitation intensity regions of active thunderstorms south through west-northwest of KSC.

ALT KFT | MAX = 570BZ, ALT = 19KFT, (AZ/R) = 341/ 24 | 07/29/94 19:48



227

Figure 5-1. South-north cross-section of thunderstorm with LDAR overlay, from 1948 UTC on day 210, 29 July 1994. Shadings indicate different radar reflectivities, though the colors have not reproduced well in black and white. Dots represent LDAR data points within the same volume scanned by the radar.

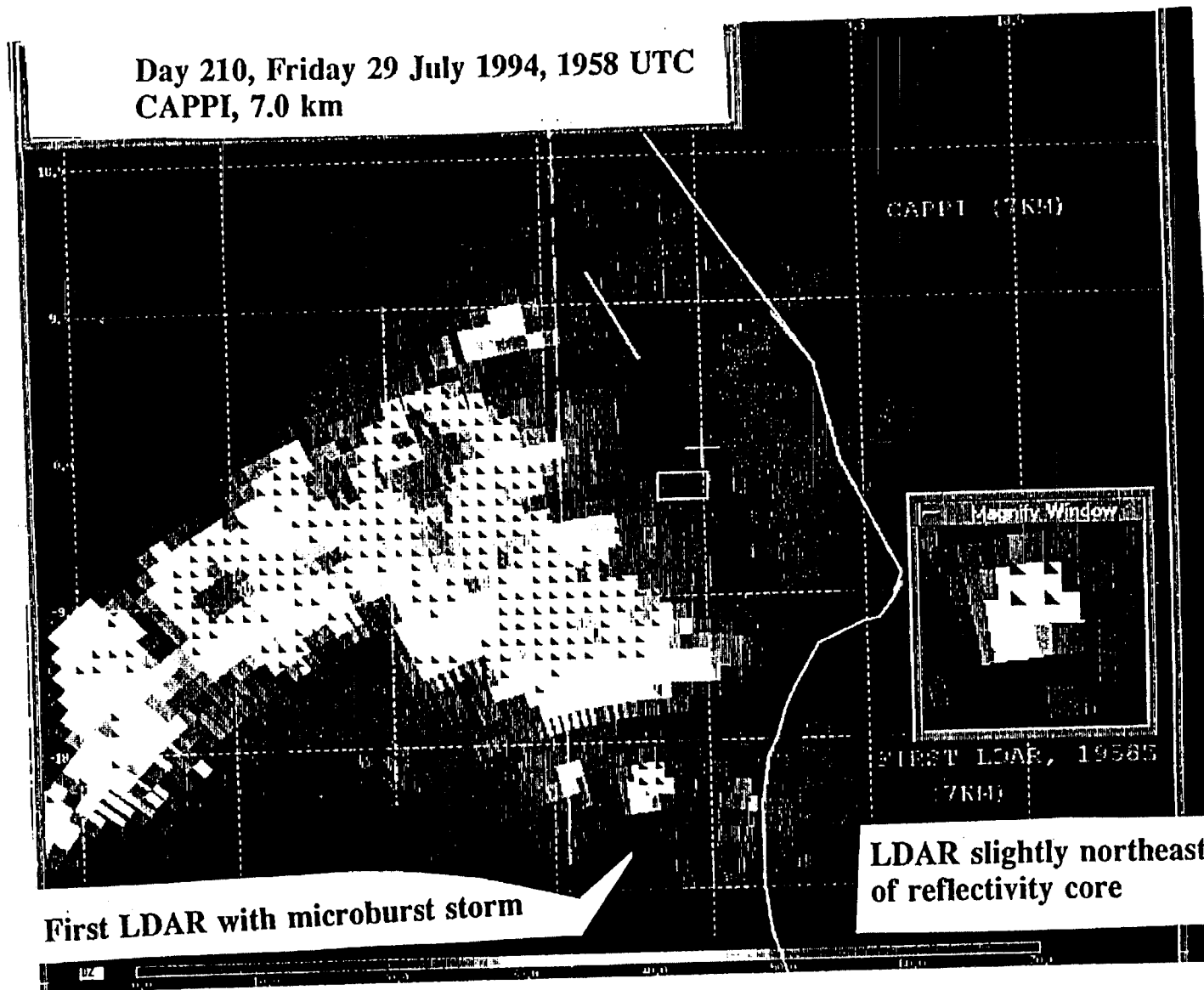


Figure 5-2. Constant-altitude display of radar reflectivities with LDAR overlay (triangles) at 7 km from 1958 UTC on day 210, 29 July 1994. Gray regions inside of white areas have highest reflectivities, about 60 dBZ.

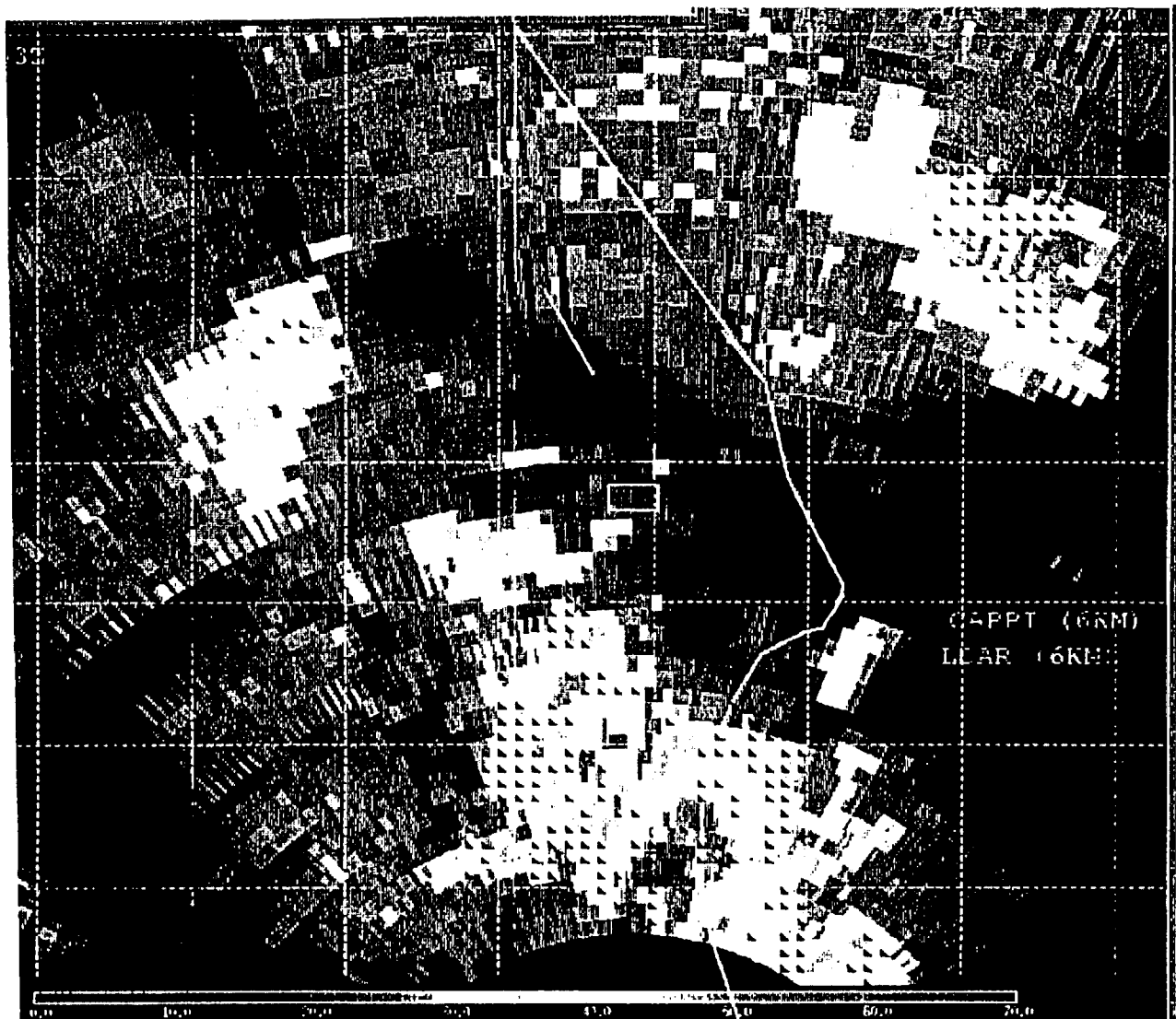


Figure 5-3. Constant-altitude display of radar reflectivities with LDAR overlay at 6 km from 2153 UTC on day 210, 29 July 1994 at 6.0 km. Reflectivities are now mostly 40 dBZ or less, except in a 60 dBZ core offshore about 10 km south of Cape Canaveral. A broad, diffuse flash extends to the west-northwest within quasi-stratiform echo rearward of that storm.

Figure 5-3 shows an example of a radar image with LDAR overlay at a later time, 2153 UTC, at 6 km. At this stage of the episode, many of the strong convective towers have weakened or disappeared, and the remaining precipitation is becoming more stratiform. LDAR activity is becoming organized into progressively more diffuse layers, with occasional quasi-horizontal branching flashes extending even tens of kilometers. One of these is depicted in the lower half of the figure. Presumably these flashes are in association with electrified cloud layers generated earlier in the day and left behind after the active portions of the storms have decayed or exited the region. However, the pockets of higher reflectivity within these regions still suggest that there may be pockets of upward vertical velocity and modest charge generation processes in progress.

## 5.2 KSC WIND PROFILER VERTICAL VELOCITIES IN RELATION TO A LAYERED LDAR STRUCTURE

Time-height series of vertical velocities measured by the KSC wind profiler confirm the existence of pockets of upward motion in the stratified cloud of the type mentioned in discussion of Fig. 5-3. Thunderstorm cells on 29 July 1994 moved toward the north-northeast, such that the cores of the major cells of Fig. 5-2 took a track passing west of the KSC wind profiler, located just east of the north end of the Shuttle Landing Facility. Thus, for much of the time the wind profiler site was under the influence of anvil and stratified debris clouds east of the thunderstorm cores.

Figure 5-4 shows the time-height section of LDAR events within 1 km of the wind profiler site as a function of time during the afternoon of 29 July 1994. Superimposed on the figure are outlines of discernible upward velocities, together with arrows showing locations of maximum upward and downward vertical motions. During the period between about 2005 and 2130 UTC, two layers of LDAR events existed over the profiler site, descending with time. The layers were initially centered near 12 and 8 km and descended to below 9 and 5 km, respectively, while becoming more diffuse. This descent could be affiliated with the fallout of charged ice crystals slowly descending from aloft. The mean descent rate is about 0.8 m/s, somewhat less than the fallspeed of ice crystals, however.

Evident in Fig. 5-4 is that the pattern of upward vertical velocities also slopes downward with time, parallel to the LDAR layers. The LDAR layers are generally affiliated with updraft, though somewhat cellular in nature. Between the layers there was a rather continued downward motion. The presence of updraft in association with the LDAR layers may explain why the net layer descent rate was slower than ice crystal terminal velocities if, indeed, that is the meteorological context. The presence of cellular updrafts within the quasi-stratiform region may also explain the dynamics through which the layers were able to remain electrically active. Additional investigation is merited.

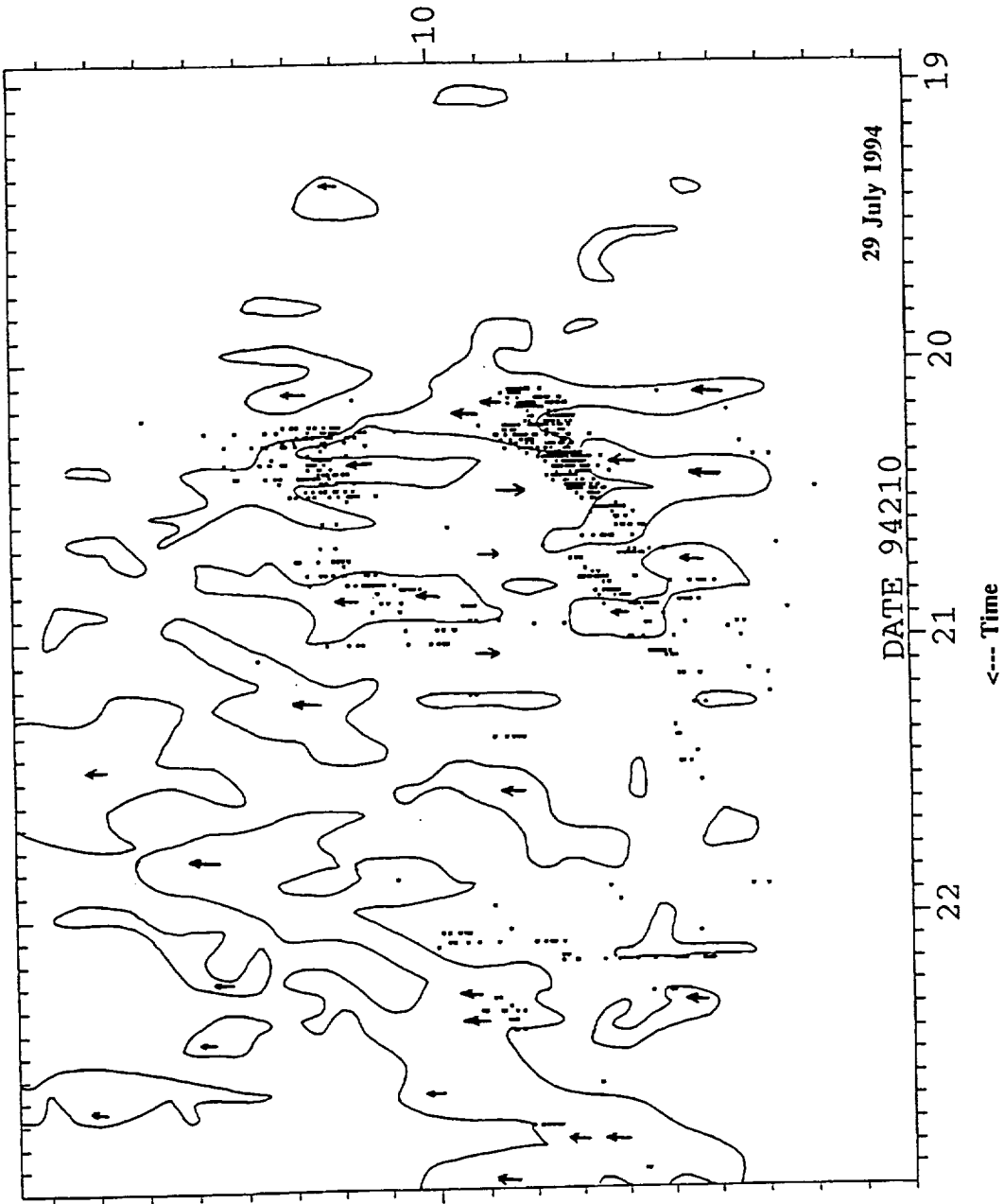


Figure 5-4. Time-height section of LDAR events above the KSC wind profiler and outlined areas of discernible upward vertical velocities between about 1900 and 2300 UTC on day 210, 29 July 1994. Arrows depict vertical velocity maxima, which peaked at 3.3 m/s.

## VI. CONCLUDING REMARKS

The task of issuing lightning advisories is a formidable one, involving a diversity of situations. In some instances the forecast problem is one of anticipating the time and location of formation of the first thunderstorm cells of the day, or determining when and if new cells will form near a forecast site, given that storms already exist elsewhere. At other times the problem is one of anticipating the movement, growth, merger, flanking cell development, or dissipation of existing thunderstorms. Yet another problem arises in knowing when and if to cancel lightning advisories while, because of vertical wind variations or other factors such as mesoscale convective systems, electrified clouds persist over a site adjacent to or following the passage of deep thunderstorm cells. The nature of the forecast problem can evolve rapidly during the day, and can be different in one weather regime from another. The forecasters are to be congratulated for their successes in a difficult job.

Operational weather forecasters involved with the space program have at their disposal a host of tools helpful in solving the above problems: radar, satellite, LDAR, field mills (LPLWS), LLP, surface mesonet (wind towers), soundings, wind profiler, and even mesoscale numerical model forecast data. Each of these platforms can contribute useful information individually. Because of the deadlines of operational decision-making, forecasters often may not have time to leisurely contemplate the interrelationships and complementary natures of these diverse pieces of information, or to re-examine past cases for clues toward future success. The goal of this ongoing research is to supplement the efforts of the forecasters by developing guidelines, approaches, and techniques involving diverse types of data that can be useful in operational weather forecasting. Based upon the studies to date, the author has given presentations to operational forecasters and provided software and training materials for use in ongoing technology transition activities.

The author looks forward to a continuing cooperation with NASA, the Applied Meteorology Unit, the National Weather Service, and other groups also performing studies with similar goals. A meeting of the participants was held in early August as a first step in coordinating these efforts.

## REFERENCES

1. Maier, M.W., A.G. Boulanger, and R.I. Sax: An initial assessment of flash density and peak current characteristics of lightning flashes to ground in South Florida. NUREG/CR-1024, U.S. Nuclear Regulatory Commission, 1979.
2. MacGorman, D.R., M.W. Maier, W.D. Rust: Lightning strike density for the contiguous United States from thunderstorm duration records. NUREG/CR-3759, U.S. Nuclear Regulatory Commission, 1984.
3. Maier, L.M., E.P. Krider, and M.W. Maier: Average diurnal variation of summer lightning over the Florida Peninsula. *Mon. Weather Rev.*, 112(6), June, 1984, pp. 1134-40.
4. Krider, E.P., A.E. Pifer and D.L. Vance: Lightning direction-finding system for forest fire detection. *Bull. Amer. Meteorological Soc.*, 61, 1980, pp. 980-86.
5. Lennon, C. and L. Maier: Lightning mapping system. NASA CP-3106, Vol, II, 1991 International Aerospace and Ground Conference on Lightning and Static Electricity, 1991, pp. 89-1 to 89-10.
6. Forbes, G.S.: Lightning studies using LDAR and LLP data and applications to weather forecasting at KSC. 1993 Research Reports, NASA/ASEE Summer Faculty Fellowship Program (C.R. Hosler, C. Valdes, T. Brown, eds.), NASA CR-194678, Grant NGT-60002 Supplement 11, 1993, pp. 165-194.
7. Holle, R.L., A.I. Watson, R.E. Lopez, R. Ortiz: Meteorological aspects of cloud-to-ground lightning in the Kennedy Space Center region. Preprints, AIAA 26th Aerospace Sci. Meeting, Reno, NV, 1988, 12pp.
8. Uman, M.A.: *The Lightning Discharge*. Academic Press, NY, 1987, 377pp

